Behavioral/Systems/Cognitive

The Representation of Stimulus Orientation in the Early Stages of Somatosensory Processing

Sliman J. Bensmaia,[1,2] Peter V. Denchev,[1] J. Francis Dammann III,[1] James C. Craig,[3] and Steven S. Hsiao[1,2]

[1]Krieger Mind/Brain Institute and [2]Department of Neuroscience, The Johns Hopkins University, Baltimore, Maryland 21218, and [3]Department of Psychological and Brain Sciences, Indiana University, Bloomington, Indiana 47405

At an early stage of processing, a stimulus is represented as a set of contours. In the representation of form, a critical feature of these local contours is their orientation. In the present study, we investigate the representation of orientation at the somatosensory periphery and in primary somatosensory cortex. We record the responses of mechanoreceptive afferents and of neurons in areas 3b and 1 to oriented bars and edges using a variety of stimulus conditions. We find that orientation is not explicitly represented in the responses of single afferents, but a large proportion of orientation detectors (~50%) can be found in areas 3b and 1. Many neurons in both areas exhibit orientation tuning that is preserved across modes of stimulus presentation (scanned vs indented) and is relatively insensitive to other stimulus parameters, such as amplitude and speed, and to the nature of the stimulus, bar or edge. Orientation-selective neurons tend to be more SA (slowly adapting)-like than RA (rapidly adapting)-like, and the strength of the orientation signal is strongest during the sustained portion of the response to a statically indented bar. The most orientation-selective neurons in SI are comparable in sensitivity with that measured in humans. Finally, responses of SI neurons to bars and edges can be modeled with a high degree of accuracy using Gaussian or Gabor filters. The similarity in the representations of orientation in the visual and somatosensory systems suggests that analogous neural mechanisms mediate early visual and tactile form processing.

Key words: **macaque; orientation; psychophysics; somatosensory cortex; tactile; tuning**

Introduction

The perceptual decomposition of a stimulus into local contours is one of the earliest stages in form processing. In the standard view, a population of neurons acts as a bank of "feature detectors," selective for the orientation of contours impinging on a specific region of the receptor sheet. Orientation tuning has been documented in SI neurons in only a few studies (for review, see Hsiao et al., 2002). Pubols and Leroy (1977) described cells in the primary somatosensory cortex of raccoon that responded preferentially to bars applied at a particular orientation. In monkey, Hyvärinen and Poranen (1978) found neurons in area 2 that were orientation selective but none in areas 3b and 1 (note, however, that the sample size was small). In another study on awake monkey (Warren et al., 1986), a small number of SI neurons (~3%) were found to respond differentially to gratings differing in orientation. Subsequently, DiCarlo and Johnson (2000) found a large proportion of neurons in area 3b that exhibited orientation tuning (39%). Although the responses of some SI neurons have been shown to be modulated by stimulus orientation, the degree to which an explicit and faithful representation of orientation exists in SI remains to be fully characterized.

In a paired psychophysical study (Bensmaia et al., 2008), we characterized the ability of human observers to both identify the orientation of and discriminate between bars and edges under a variety of stimulus conditions. We found that to reliably discriminate differences in orientation requires a change of ~20°. We also examined a number of stimulus factors to determine their effect on orientation acuity, and found it to remain relatively unchanged with variations in such factors as stimulus amplitude, duration, bar length, and presentation mode (indented or scanned).

In the present study, we characterize the responses of mechanoreceptive afferents and of neurons in areas 3b and 1 to stimuli similar to or identical with those used in the psychophysical experiments. One of the aims of the present study is to determine the extent to which orientation-sensitive neurons can be considered "feature detectors." A critical question is whether the responses of neurons in primary somatosensory cortex to oriented stimuli exhibits invariance across stimulus manipulations. Stimulus manipulations included the type of stimulus, bar or edge, the mode of presentation, scanned or indented, the scanning speed, and the amplitude of the stimulus. We characterize the ability of each neuron to convey information about stimulus orientation, and the degree to which the orientation signal is sensitive to other stimulus parameters. To investigate whether form is processed within a distinct pathway, which originates in slowly adapting type 1 (SA1) afferents at the somatosensory periphery, we as-

Received Sept. 11, 2007; revised Nov. 14, 2007; accepted Dec. 6, 2007.

This work was supported by National Institutes of Health Grants NS-18787, NS-34086, and DC-00095. We thank Justin Killebrew for his invaluable technical assistance. We also express our gratitude to Supratim Ray, Pramod Thakur, and Jeffrey Yau for stimulating discussion.

Correspondence should be addressed to Sliman J. Bensmaia, Krieger 338, 3400 North Charles Street, Baltimore, MD 21218. E-mail: sliman@jhu.edu.

DOI:10.1523/JNEUROSCI.4162-07.2008

 0270-6474/08/280776-11$15.00/0

sessed whether the adapting properties of the neuron [i.e., slowly adapting (SA) or rapidly adapting (RA)] are predictive of its sensitivity to orientation. We also evaluated the degree to which the orientation signal in SI can account for psychophysical performance. Finally, we investigated the neural mechanisms of orientation selectivity using simple receptive field (RF) models.

Materials and Methods

Stimuli

Stimuli were generated and delivered with a device consisting of 400 independently controlled pins arrayed over a 1 cm^2 area (Killebrew et al., 2006). This array permits us to generate complex spatiotemporal patterns that simulate the kind of stimulation generated by a finger contacting a surface.

Indented bars or edges

On each trial, a bar or edge was indented into the skin at one of eight orientations, ranging from 0 to 157° in steps of 22.5° with 0° defined as the orientation perpendicular to the long axis of the finger. The amplitude (or depth of indentation) of the bar was 500 μm, its width was 1 mm, and its duration was 100 ms. (The duration of indented stimuli was 50 ms when recording from peripheral afferents.) Edges were defined similarly except that all of the probes were at 500 μm on one side of the edge. The pivot of the bar (or edge), which was also its center, was located either at the point of maximum sensitivity (or hotspot) of the neuron or was offset relative to the hotspot by 1–4 mm in the axis normal to the orientation of the bar. The interstimulus interval was 100 ms. Bars (or edges) were each presented 10 times in pseudorandom order for a total of 720 trials (8 orientations × 9 locations × 10 presentations).

Scanned bars and edges

On each trial, a bar or edge was scanned across the skin. The scanning direction (two per orientation) was perpendicular to its orientation, which assumed one of eight values ranging from 0 to 157° in 22.5° steps. Scanning direction thus ranged from 0 to 337.5° in 22.5° steps. The amplitude of the bars was 300, 500, or 700 μm and their width was 1 mm, and the amplitude of the edges was 500 μm. The scanning velocity for all stimuli was 40 mm/s and the interstimulus interval was 200 ms. Bars were each presented five times in pseudorandom order for a total of 240 trials (8 orientations × 2 scanning directions/orientation × 3 amplitudes × 5 presentations). Edges were each presented 10 times in pseudorandom order (except that leading and trailing edges were interleaved) for a total of 160 trials (10 presentations each of leading edges at 8 orientations and trailing edges at 8 orientations).

From the responses of the neuron to scanned bars, we established its preferred direction and orientation (i.e., the orientation and direction at which its response was maximal). In a subsequent set of measurements, bars were scanned in the preferred and antipreferred direction (i.e., bars at the same orientation but moving in opposite directions), as well as in the two orthogonal directions. The amplitude of the bars was 500 μm, and their width, 1 mm. The scanning velocity was 10, 20, 40, or 80 mm/s. Bars were each presented five times in pseudorandom order for a total of 240 trials (2 orientations × 2 scanning directions/orientation × 3 amplitudes × 4 velocities × 5 presentations).

Single-probe indentations

This protocol was used to identify the hotspot of the neuron and the spatial extent of its RF. On each trial, one of the 400 probes was indented into the skin for 100 ms at an amplitude of 300 μm. The duration of the on- and off-ramps was 25 ms (as was the case for all indentation protocols) and the interstimulus interval was 100 ms. Successively indented probes were never adjacent to minimize effects of skin dynamics.

Multiple-probe indentations

This protocol was used to gauge the extent to which individual neurons were slowly or rapidly adapting (see below). On each of 60 trials, nine probes, arrayed in a 3 × 3 square and centered on the RF of the neuron, were indented into the skin for a duration of 0.5 s, and then retracted for a duration of 0.5 s.

Neurophysiology

Peripheral experiments

All experimental protocols complied with the guidelines of The Johns Hopkins University Animal Care and Use Committee and the National Institutes of Health's *Guide for the Care and Use of Laboratory Animals*. Single-unit recordings were made from the ulnar and median nerves of four macaque monkeys (*Macaca mulatta*) using standard methods (Talbot et al., 1968). Standard procedures were used to classify mechanoreceptive afferents according to their responses to step indentations (Talbot et al., 1968; Freeman and Johnson, 1982). An afferent was classified as SA1 if it had a small RF and produced sustained firing in response to a step indentation. It was classified as RA if it had a small RF and responded only to the onset and offset of an indentation. It was classified as Pacinian (PC) if (1) it was vigorously activated by air blown gently over the hand, (2) it was activated by transmitted vibrations produced by tapping on the hand restraint, and (3) its RF was large. The point of maximum sensitivity of the afferent (or hotspot) was located on the skin using a handheld probe and then marked with a felt-point pen. The stimulator probe was centered on the point of maximum sensitivity (or hotspot) of the afferent. We recorded from an afferent only if its RF was located on the distal fingerpad of digits 2–5 and if the probe could readily be centered on the RF. We did not record responses from PC afferents because these have been shown to be highly insensitive to the spatial properties of stimuli presented to their RFs (Johnson and Lamb, 1981).

Cortical experiments

Extracellular recordings were made in the postcentral gyri of one hemisphere of three macaque monkeys using previously described techniques (Mountcastle et al., 1991). On each recording day, a multielectrode microdrive (Mountcastle et al., 1991) was loaded with seven quartz-coated platinum/tungsten (90/10) electrodes (diameter, 80 μm; tip diameter, 4 μm; impedance, 1–3 MΩ at 1000 Hz). The microdrive proboscis was inserted into a recording chamber filled with physiological saline and oriented so that the electrodes were normal to the skull. The electrodes were then driven into the cortex until they encountered neurons in area 1 with RFs on the distal fingerpad. A day spent recording from area 1 was typically followed by a day spent recording from area 3b. When recording from area 3b, the electrodes were driven 2–3 mm below the top of the neural activity until neurons with RFs on the distal fingerpad were encountered. Because electrodes were aligned perpendicularly to the central sulcus, signals on multiple electrodes were often evoked from overlapping regions of skin. In these cases, we recorded from more than one electrode. Many of our experimental protocols were adaptive. Thus, although multiple neurons could be recorded from, one neuron was selected, usually based on the quality of its isolation, as the principal neuron to which individual stimulus protocols were tailored (see above).

The transition from area 1 to area 3b exhibits a characteristic progression of RF locations. As one descends from the cortical surface through area 1 into area 3b, the RFs progress from the distal, to middle, to proximal finger pads, and then to the palmar whorls. Within area 3b, the RFs proceed back up the finger, transitioning from proximal, to medial, and ultimately to distal pads. Because responses from the distal pad were never encountered in the more superficial regions of 3b (where the palmar whorls or proximal pad typically were most responsive), there was never any uncertainty about the anatomical area from which the neurons originated.

We recorded from neurons whose RFs were located on the distal pads of digits 2–5. On every second day of recording, the electrode array was shifted ~200 μm along the postcentral gyrus until the entire representation of digits 2–5 had been covered. At the end of the recording day, the electrodes were withdrawn and a few drops of dexamethasone, as well as a drop of gentamicin ophthalmic solution, were applied to the dura. The dura was then covered with Gelfoam and the chamber was filled with sterile saline and sealed.

Recordings were obtained from neurons in areas 3b and 1 that met the following criteria: (1) action potentials were well isolated from the background noise, (2) the RF of the neuron included at least one of the distal finger pads on digits 2–5, (3) the stimulator array could be positioned so that the RF of the neuron was centered on the array, and (4) the neuron

was clearly driven by one or more of the initial protocols (namely, RF mapping, direction selectivity, and scanned bars). Because we tailored the stimuli to the responses of a single neuron (see above), it was imperative that the isolation be sustained for an extended period of time (1.25–1.5 h). We thus were very particular as to isolation quality.

Analysis

Identification of the RF center

From the RF mapping protocol, we plotted the mean response (averaged across the five presentations of the stimulus) as a function of pin position. We then selected as hotspot the region of highest driving of the RF. All indented stimuli were then presented at or around this position on the 400-probe array as described above.

Adaptation index

One issue we wanted to address was whether the adapting properties of neurons (i.e., whether they adapted slowly or rapidly) were predictive of their sensitivity to stimulus orientation. RA neurons tend to produce responses only during the transient portion of an indented stimulus (onset and offset), whereas SA neurons produce a response during the sustained portion of the stimulus as well. We thus computed an "adaptation index" (i.e., the proportion of the total response that occurs after the offset of the stimulus). The index was derived from data obtained in the SA/RA protocol, which consists of a series of 500 ms indentations interleaved with 500 ms empty intervals. Because both SA1 and RA afferents produce (on-) responses at the onset of the stimulus, we excluded the first 100 ms of the response from the analysis, because this response period does not discriminate between these two populations of fibers. The response evoked during the first 100 ms after stimulus offset was divided by the response obtained during the entire stimulus (excluding the on-response and correcting for response latency, defined as the time of steepest rise in the neural response). (We found this to be a robust measure of response latency. To correct for latency, we subtracted the estimated response latency from the time of occurrence of each spike.) The baseline firing rate of the neuron was measured from its responses during the 400 ms interval before each stimulus. The index was computed after the baseline firing rate had been subtracted from the stimulus-evoked responses. If a cell was an ideal RA neuron, the adaptation index was 1, because the neural response (excluding the on-response) was confined to the period immediately after the offset of the stimulus. If a cell were an idealized SA neuron, then the adaptation index would be 0, because the neuron was silent after the offset of the stimulus. This index yields a perfect dichotomization of SA1 and RA responses at the somatosensory periphery.

Measurement of the response to scanned and indented bars

Because not all stimuli overlapped the RF of a neuron during the entire stimulus interval, steps were taken to ensure that neural responses were measured over the period during which the stimulus was impinging on the RF of the cell. Specifically, the response to a scanned bar was measured over a 100 ms interval centered around the time at which the bar passed over the hotspot of the neuron. We used responses to scanned bars rather than to indented probes to identify the hotspot of each neuron because a subset of neurons responded to the former but not the latter.

To locate the hotspot, we first identified the time at which a bar scanned in each of the 16 directions passed over a given location on the array. We then computed the response of the neuron over a 100 ms time window centered on the appropriate time for the corresponding bar, correcting for the response latency (estimated from the neural responses obtained in the SA/RA protocol). Finally, we averaged the response of the neuron to bars at all orientations as they passed across this location on the array. We repeated this procedure for every location on the array (sampling in 100 μm steps along both axes). From this response map, we identified the location on the array that yielded the highest response averaged across orientations. We then used the mean response over a 100 ms time window centered on this location as our measure of the response of the neuron to scanned bars. We performed analyses on neural responses to scanned bars over other time windows (25, 50, and 200 ms) to assess whether the width of the window affected our conclusions and found that it did not (over the range of windows tested). We chose a 100 ms window because (1) it corresponded to the duration of the indented bars, and (2) it was short enough that the bars remained within the RF of most neurons (whose RF diameter tends to be >4 mm) while maximizing the interval over which responses were averaged (thereby minimizing the noise).

Because, more often than not, we recorded the responses of a single neuron at a time, one set of bars was tailored to that neuron and centered on its RF. Nonetheless, indented bars at a given orientation were presented at a total of nine locations on the array, centered on the RF of the principal neuron (see above). For every other neuron, responses to the bar that was nearest to its hotspot (measured from scanned bars as described above) were used to characterize its orientation selectivity.

Index of orientation selectivity

As an index of orientation selectivity, we used vector strength as follows:

$$o_i = \frac{\sqrt{\left[\sum_i R(\theta_i) sin(2\theta_i)\right]^2 + \left[\sum_i R(\theta_i) cos(2\theta_i)\right]^2}}{\sum_i R(\theta_i)}, \quad (1)$$

where $R(\theta_i)$ is the response of the neuron to a bar at orientation θ_i. We computed o_i for each neuron in each presentation mode (Mardia, 1972). Values of o_i could range from 0, when a neuron responded uniformly to all orientations, to 1, when a neuron only responded to stimuli at a single orientation. The statistical reliability of o_i was tested using a standard randomization test ($\alpha = 0.01$). For a discussion contrasting o_i (which is 1 − the circular variance) and other indices of orientation selectivity, see Ringach et al. (2002).

The preferred orientation was determined by fitting a von Mises function, the circular analog to a Gaussian function, to the mean responses using a least-squares method. The mean of the distribution was taken to be the preferred orientation of the cell.

Characterizing the time course of the response to indented bars

We wanted to characterize the time course with which the orientation signal develops in the population of neurons in area 3b and 1. Because indices of orientation selectivity are highly unstable for sparse responses [like those expressed in poststimulus spike histograms (PSTHs) with small bin sizes], responses were pooled across neurons. Specifically, the strength of the orientation signal was characterized by comparing the responses of all neurons at their respective preferred orientations to their responses at the corresponding orthogonal orientations.

First, we smoothed the PSTH (bin size, 1 ms) obtained at the preferred orientation of each neuron and at the orthogonal orientation using a third-order Savitzky–Golay polynomial smoothing filter with a length of 25 ms. We then separately averaged the filtered spike trains at the preferred and orthogonal orientations across neurons for each time interval and computed from these mean smoothed PSTHs the following index of orientation selectivity:

$$o_i^*(t) = \left| \frac{\overline{R_{\phi_p}(t)} - \overline{R_{\phi_{np}}(t)}}{\overline{R_{\phi_p}(t)} + \overline{R_{\phi_{np}}(t)}} \right|, \quad (2)$$

where $\overline{R_{\phi_p}(t)}$ is the mean response of all orientation selective neurons to their preferred orientation, ϕ_p, and $\overline{R_{\phi_{np}}(t)}$ is the mean response to the orthogonal orientation, ϕ_{np}, at time t. We also computed the filtered PSTH, averaged across the two orientations, to characterize the timing of the on- and off-responses in the population response.

Computation of neurometric functions

We estimated the ability of individual neurons to signal changes in orientation using an ideal observer analysis. For each neuron, we randomly sampled, with replacement, from one of the 10 neural responses evoked at the preferred orientation and one of the 20 neural responses evoked at an orientation shifted by $\Delta\phi$ degrees (there were 10 presentations of each stimulus and we assumed that $\pm\Delta\phi$ are equivalent). We repeated this

procedure 1000 times and computed the proportion of times the response was greater at the preferred orientation than when the orientation was shifted by $\Delta\phi$. Thus, to obtain the relative distributions of neural responses at ϕ_p and $\phi_p \pm 22.5°$ evoked in a cell whose preferred orientation was 90°, we sampled, on each of 1000 iterations, one response evoked by a 90° bar and one response to a bar oriented either at 67.5 or 112.5° and computed the proportion of times the former was larger than the latter. The angular threshold of a neuron was defined as the difference $\Delta\phi$ such that the response to a bar at the preferred orientation, ϕ_p, was stronger than the response to a bar oriented at $\phi_p \pm \Delta\phi$ 75% of the time. Neurometric functions obtained from inhibitory neurons were inverted. A sigmoid function was fit to each neurometric function to obtain an estimate of the width of tuning for that neuron (which was the SD of the sigmoid).

Assessing the linearity of neural responses to indented bars

A basic model relating a stimulus to the neural response it evokes is one that assumes that the neuron acts as a linear spatial filter, the output of which is passed through a nonlinear transformation. According to this framework, stimulation of each patch of skin leads to an increase or a decrease in the response of the neuron, or has no effect; the response of the neuron is determined by the sum of the effects produced by stimulation of individual skin patches. The nonlinear transformation we adopted was a half-wave rectified linear function. We tested four linear models.

Punctate probe RF. We used the RF map, measured using punctate probes (see above), as an estimate of the linear filter of the neuron. To generate model predictions, we convolved the (measured) punctate probe RFs with the displacement profile of each of the 72 indented bars (8 orientations, 9 locations per orientation), and then scaled and rectified the output of the convolution.

Punctate probe RF using the strain profile. To determine the degree to which the nonlinearity was attributable to skin mechanics, we tested the hypothesis that neural responses were linear with the strain profile. To that end, we computed the strain profile (Sripati et al., 2006),[a] convolved this strain profile with the punctate probe RF of each neuron, and then scaled and rectified the output of the convolution.

Gaussian filter. We tested whether the RF structure of neurons could be approximated using a Gaussian filter. The filter was fit to the responses to indented bars, for each neuron individually, using a nonlinear least-squares method (lsqcurvefit, Matlab 7.1, MathWorks, Natick, MA). The model consisted of seven parameters, five characterizing the filter and two, the scaling factors. To generate model predictions of responses to indented bars, the filter was convolved with each stimulus and the output of the convolution was scaled and then rectified as follows:

$$R(S) = \left[\alpha \left[e^{-\left(\frac{u^2}{2\sigma_u^2} + \frac{v^2}{2\sigma_v^2} \right)} \right] \otimes S + \beta \right]^+,$$

$$\text{where } u = (x - x_c) \cdot \cos(\theta) + (y - y_c) \cdot \sin(\theta)$$

$$v = -(x - x_c) \cdot \sin(\theta) + (y - y_c) \cdot \cos(\theta), \quad (3)$$

and where $R(S)$ is the response to the stimulus with displacement profile S, (x_c, y_c) is the center of the filter, σ_u and σ_v are its widths along its two dimensions, and α and β are scaling factors (the last plus sign in Eq. 3 denotes half-wave rectification).

Gabor filter. The orientation selectivity of neurons in primary visual cortex is attributed to RF structures consisting of excitatory bands flanked by inhibitory ones. To assess whether this RF structure could account for orientation selectivity in SI, we modeled the RF of each neuron as a two-dimensional Gabor filter. To generate model predictions of responses to indented bars, the filter was convolved with each stimulus and the output scaled then rectified. The nine parameters of the model

[a]To obtain the strain profiles for cortical neurons (which receive input from SA1 and/or RA fibers), we computed the maximum tensile strain at a depth of 1.2 mm, the mean fitted depth across afferent types. The choice of strain component or depth had little impact on the results (for depths ranging from 0.6 to 2 mm). For SA1 fibers, we computed the maximum tensile strain at a depth of 0.8 mm; for RA fibers, we used relative change in membrane area at a depth of 1.6 mm (cf. Sripati et al., 2006).

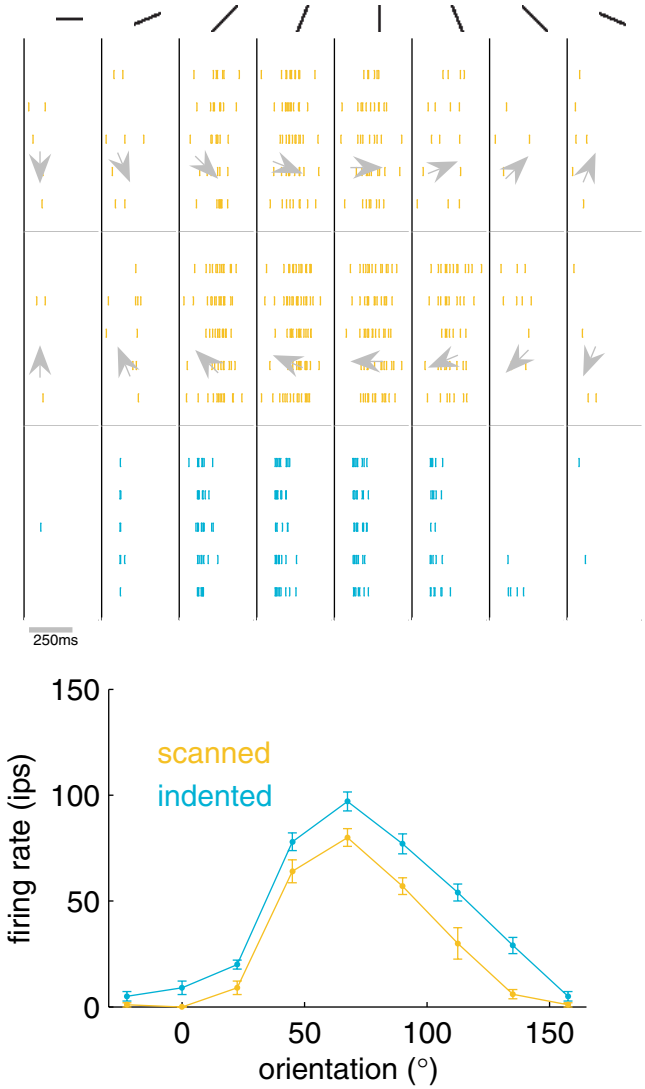

Figure 1. Top, Responses of a neuron in area 3b to scanned (orange) and indented (cyan) bars at eight orientations (0–157.5° in 22.5° increments). The amplitude of the bars was 500 μm. The duration of the scanned bars was 400 ms, and that of the indented bars was 100 ms. The gray arrows denote the direction in which bars were scanned. Bottom, Tuning curves derived from the same cell. The preferred orientation of this strongly tuned cell ($o_i = 0.65$) is consistent across presentation modes, scanned and indented. Error bars indicate SEM.

(α, β, γ, ϕ, λ, σ, θ, x_c, and y_c) were fit to the responses of each neuron using a nonlinear least-squares method as follows:

$$R(S) = \left[\alpha \left[e^{-\frac{(u^2+\gamma^2v^2)}{2\sigma^2}} \cos\left(\frac{2\pi \cdot u}{\lambda} + \phi \right) \right] \otimes S + \beta \right]^+ \quad (4)$$

(see above for conventions).

For each of the four models, we computed the correlation between model predictions and the mean responses to each of the 72 stimuli and squared it to obtain the coefficient of determination, R^2, which represents the proportion of variance in the neural responses explained by the model.

Results

Responses to scanned and indented bars

We recorded the responses of 132 neurons in primary somatosensory cortex (63 in area 3b and 69 in area 1) and 31 mechanoreceptive afferent fibers (20 SA1 and 11 RA). Figure 1 shows the responses of a strongly orientation-selective neuron in area 3b to scanned and indented bars with amplitudes of

500 μm. This neuron exhibited a characteristic tuning to stimulus orientation: Its response was strongest to bars oriented at 67.5° (i.e., 22.5° clockwise rotation from the long axis of the finger) and decreased as the bars were rotated away from this orientation. Importantly, the preferred orientation was the same for scanned and indented bars and was independent of scanning direction. The orientation tuning of this cell was also independent of the amplitude of the stimulus: Although the response to indented bars increased with increasing stimulus amplitude, the tuning was identical across amplitudes (Fig. 2*A*). Figure 2, *B–D*, shows the amplitude independence of the tuning of three other cortical neurons.

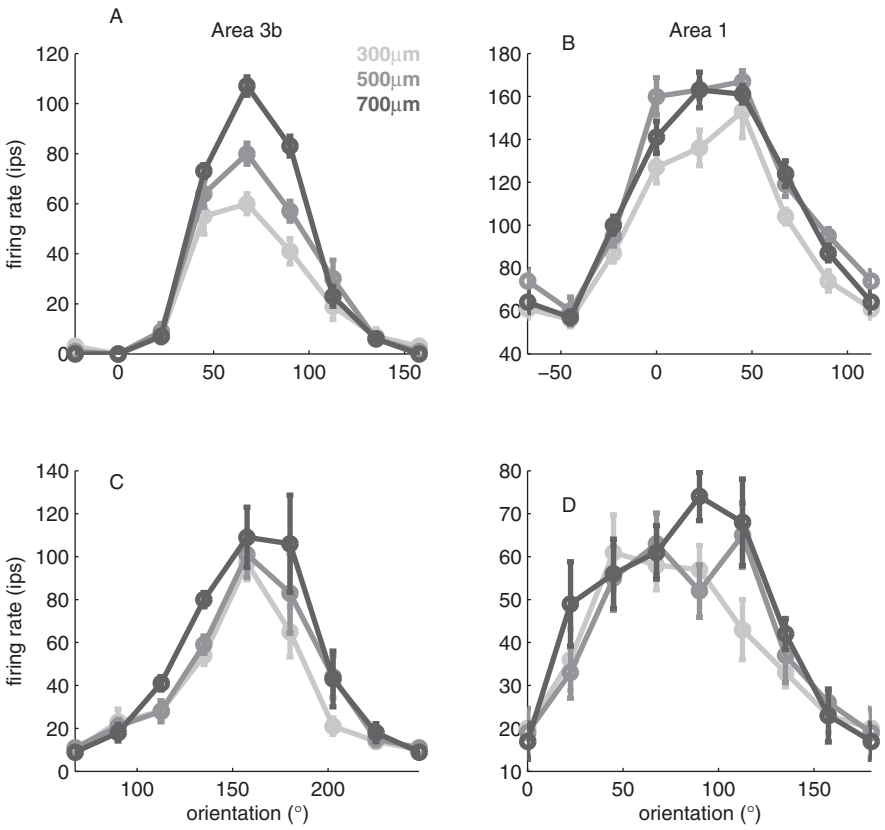

Figure 2. Effect of stimulus amplitude on the responses of two neurons in area 3b (***A***, ***C***) and two neurons in area 1 (***B***, ***D***) to scanned bars. The 500 μm trace in the top left panel is the same as that shown in Figure 1. The orientation tuning of the response was relatively independent of stimulus amplitude; the mean o_i increased from 0.39 to 0.43 as the amplitude increased from 300 to 700 μm. Furthermore, increasing the stimulus amplitude had little effect on the overall response for three of the four neurons shown. Error bars indicate SEM.

Figure 3 shows the cumulative distributions of the orientation indices, o_i, derived from the responses of SA1 and RA afferents and of neurons in areas 3b and 1 to scanned and indented bars. As can be seen from the figure, mechanoreceptive afferents exhibited little or no orientation tuning. The magnitude of the tuning was in all cases small ($o_i < 0.15$). In some cases, however, the o_i for peripheral fibers was significantly >0 because the responses were highly repeatable: 14 (of 31) afferents yielded significantly orientation-tuned responses to indented bars, and 16 yielded significantly tuned responses to scanned bars ($p < 0.01$). SA1 fibers tended to be more orientation selective to both indented and scanned bars than their RA counterparts: Only 3 (of 11) RA fibers exhibited significantly orientation-selective responses to indented bars and 4 to scanned bars, whereas 11 (of 20) SA1 afferents produced significantly orientation-tuned responses to indented bars and 12 to scanned bars. The slight orientation selectivity observed in afferents is likely attributable to the eccentricity of their RFs. Indeed, mechanoreceptive afferents have elliptical RFs, which can give rise to orientation-tuned responses. Although individual afferents do not convey a robust orientation signal, the population of mechanoreceptive afferents conveys an isomorphic spatial image of the stimulus from which orientation information can be extracted (Fig. 4). Importantly, SA1 fibers tend to convey a more acute spatial image than do RA afferents (Phillips and Johnson, 1981a; LaMotte and Srinivasan, 1987a,b; Srinivasan and LaMotte, 1987) despite the fact that they less densely innervate the skin (Vallbo and Johansson, 1978; Darian-Smith and Kenins, 1980).

Cortical neurons were significantly more orientation selective than were peripheral afferents ($t_{(102)} = 4.4$, $p < 0.001$). For indented bars, 52% (16 of 31) of the cells in area 3b and 64% (30 of 47) of the cells in area 1 were significantly orientation selective ($p < 0.01$), and the distributions of o_i were not significantly different across anatomical areas (Kolmogorov–Smirnov test: $K = 0.20, p > 0.4$). For scanned bars, 25% (16 of 63) of the cells in area 3b were significantly orientation selective compared with 52% (36 of 69) in area 1, and the difference between areas was significant ($K = 0.29, p < 0.01$).[b]

Among the subset of neurons that were tested with both scanned and indented bars, 39% (12 of 31) of the cells in area 3b and 49% (23 of 47) of the cells in area 1 were significantly orientation selective for both scanned and indented bars. The degree of orientation selectivity of these cells, as gauged by o_i, was significantly higher for indented than scanned bars (paired *t* test: $t_{(34)} = 2.1$, $p < 0.05$). The tuning widths (estimated from neurometric functions) were similar for neurons in both anatomical areas, and were significantly wider for scanned than indented bars (paired *t* test: $t_{(34)} = 3.71$, $p < 0.01$) (Fig. 5, bottom panels).

Importantly, the preferred orientation of significantly orientation-selective cells ($p < 0.01$) in the two presentation modes was very similar: The mean angular difference between the two measured preferred orientations was 5 and 10° for neurons in areas 3b and 1, respectively, confirming that the orientation signal carried by these neurons is the same whether the stimulus is scanned or indented, an important property for a feature detector. In addition, the preferred orientations of orientation-selective cells were uniformly distributed over the range of orien-

[b]The difference in orientation selectivity for scanned and indented bars, particularly that observed for neurons in area 3b, may in part be attributable to the fact that neural responses obtained in the two stimulus conditions were estimated differently. Indeed, the bars were indented at the hottest spot of the neuron, whereas the response to scanned bars was averaged over a travel length of 4 mm. The advantage of this method of estimating the responses to scanned bars is that the estimates were stable across stimulus presentations. The disadvantage is that the estimate may have incorporated responses evoked when the stimulus was at the periphery of the RF, where the stimulus dependence of the response may be weaker.

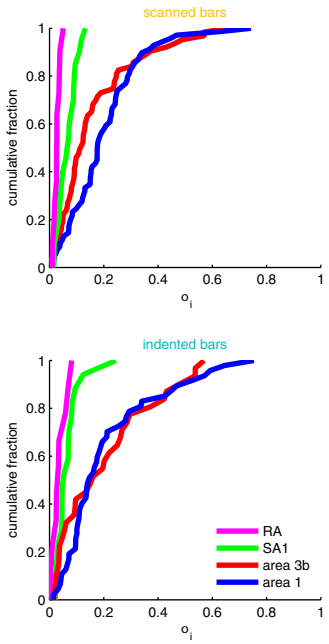

Figure 3. Cumulative distributions of the orientation index, o_i, for RA (magenta) and SA1 (green) afferents and for neurons in areas 3b (red) and 1 (blue). The amplitude of the indented bars was 500 μm and that of the scanned bars was 300 μm (the maximum amplitudes used in the experiments with mechanoreceptive afferent fibers in the two presentation modes). Afferent responses exhibited little orientation selectivity; SA1 responses were consistently more orientation selective than their RA counterparts. A large number of cortical neurons exhibited orientation-tuned responses. Orientation selectivity for indented bars was comparable in areas 3b and 1. However, more neurons in area 1 exhibited tuned responses to scanned bars.

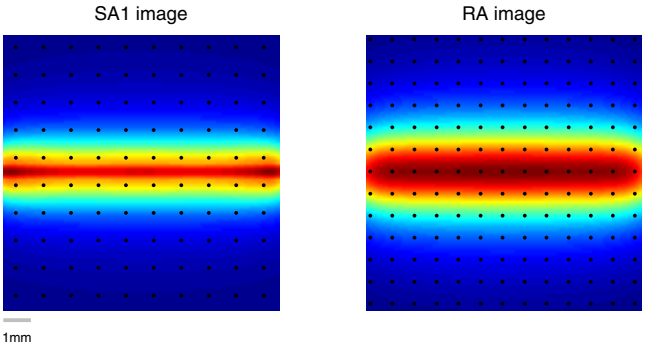

Figure 4. Representation of a horizontal bar at the somatosensory periphery as estimated using a continuum mechanical model of afferent responses (Sripati et al., 2006). The black dots show the approximate innervation density assuming a regular lattice [using densities in the human hand from Johansson and Vallbo (1979)]. The color map shows the relative activity of the afferents as a function of their position. The spatial image conveyed by SA1 afferents is sharper than that conveyed by RA afferents despite the fact that RA afferents more densely innervate the skin: The RA image is more spatially filtered than its SA1 counterpart.

tations ($K = 0.12$; $p > 0.2$) (Fig. 5, top panels). That is, there was no tendency for any one orientation to be overrepresented or underrepresented.

Orientation tuning for the population of cortical neurons was independent of stimulus amplitude over the range of amplitudes tested (from 300 to 700 μm) (Fig. 6*A*). For the subset of significantly orientation-selective neurons tested at different scanning speeds ($N = 74$; $N_{\text{area 3b}} = 27$; $N_{\text{area 1}} = 47$), the degree of orientation selectivity was found to be insensitive to the speed at which bars were scanned over the range of speeds tested (Fig. 6*B*) ($F_{(3,67)} = 0.3$ and $F_{(3,135)} = 0.91$ for neurons in area 3b and 1, respectively; $p > 0.1$).

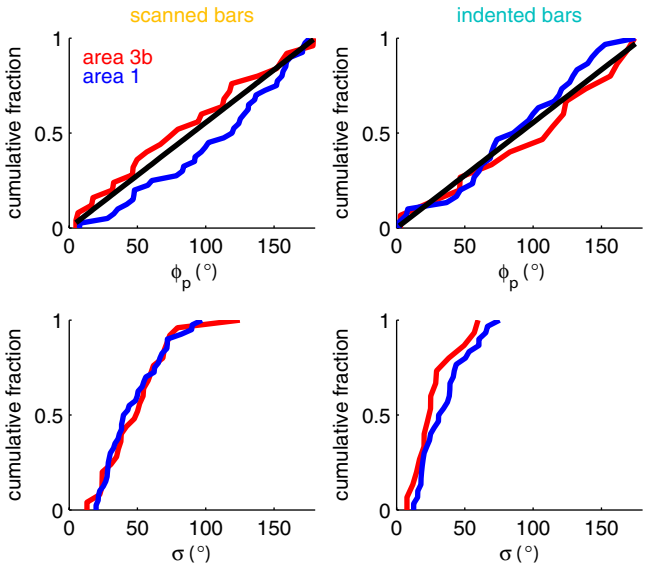

Figure 5. Top, Cumulative distributions of preferred orientations for orientation-selective neurons in areas 3b and 1 for scanned (left) and indented (right) bars. The black trace shows the expected distribution of ϕ_p if it were uniform (i.e., if all orientations were equally represented in cortex). The distributions were not significantly nonuniform (Kolmogorov–Smirnov test; scanned: $K = 0.1$ and 0.19 for areas 3b and 1, respectively; indented: $K = 0.39$ and 0.29; $p > 0.1$). Bottom, Cumulative distributions of the tuning width, computed by fitting sigmoids to the neurometric functions. The width of tuning was similar for neurons in areas 3b and 1 (mean $\sigma = 49$ and 34° for scanned and indented bars, respectively).

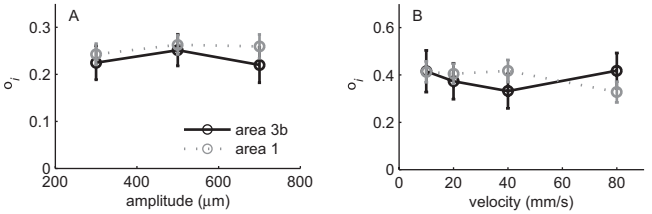

Figure 6. ***A***, Effect of stimulus amplitude on orientation selectivity for bars scanned at 40 mm/s. ***B***, Effect of scanning speed on orientation selectivity for bars of amplitude 500 μm. Error bars indicate SEM.

Responses to scanned and indented edges

The contours of an object are typically edges, which differ from the bars discussed thus far in that the object is "filled-in" on one side of the edge. Figure 7 shows the response of a neuron in area 3b to scanned edges. The preferred orientation of this neuron is the same in the two scanning conditions, leading and trailing (although the responses of this neuron to leading edges are stronger and more strongly tuned than are those to trailing edges). In a subset of neurons that were significantly orientation selective (indented: $N = 42$; scanned: $N = 51$), we compared the orientation signal evoked by edges to that evoked by bars. The orientation index, o_i, was higher for indented bars than it was for indented edges (paired t test: $t_{(41)} = 4.9$, $p < 0.01$), whereas o_i derived from responses to scanned bars and edges were not significantly different ($t_{(50)} = -0.57$ and -0.77 for leading and trailing edges, respectively; $p > 0.4$). Finally, there was no difference in o_i obtained for leading and trailing edges ($t_{(50)} = -0.34$; $p > 0.5$). The preferred orientation was typically, although not always, consistent across stimulus type: For indented stimuli, the mean differences between ϕ_p derived from responses to bars and edges was 22 and 11° for neurons in areas 3b and 1, respectively (for scanned bars,

22 and 30°; the reason for the large discrepancy for scanned bars is unclear).

Adaptation and orientation selectivity

One possibility is that form perception in cortex is mediated by a subpopulation of neurons that receives input primarily from SA1 afferents, which have been shown to mediate fine spatial processing at the somatosensory periphery (for review, see Hsiao and Bensmaia, 2007). We might then expect that orientation selectivity will be greater for SA-like neurons than for RA-like neurons. For scanned bars, the correlation between the adaptation index and the orientation selectivity index was slightly but significantly negative ($r = -0.2$; $t_{(59)} = 2.2$; $p < 0.05$), as would be predicted from this hypothesis because the adaptation index approaches 1 as the neuron becomes more RA-like. However, for indented bars, the two quantities were unrelated ($r = 0.05$; $t_{(68)} = 0.36$; $p > 0.5$). That RA input compromises the orientation selectivity for scanned bars more than it does that for indented bars is compatible with our hypothesis: RA afferents respond throughout the stimulus period for scanned bars but produce only transient responses during the onset and offset of an indented stimulus (data not shown). The interference of the less orientation-selective RA signal with the SA1 signal will therefore be more pronounced for scanned than for indented bars. This analysis suggests that slowly adapting neurons in cortex tend somewhat to be more orientation selective than rapidly adapting neurons.

RA afferents respond only at the onset and offset of a statically indented stimulus. The contribution of RA and SA1 input to the cortical orientation signal might therefore be assessed from the degree to which the on- and off-responses of cortical neurons convey information about stimulus orientation. We might then compare the strength of this orientation signal during the transient portion of the stimulus to that during the sustained portion. As can be seen in Figure 8, the strength of the orientation signal was weakest during the on- and off-responses and strongest during the sustained response. The orientation signal is strongest during the sustained portion of the stimulus because neural responses to the nonpreferred orientation were confined to the on- and off-periods to a greater extent than were responses to the preferred orientation. This temporal analysis suggests that the RA thalamocortical input does not convey a strong orientation signal. Note that the orientation signal during the on- and off-responses is not nil. In fact, some neurons whose response is entirely restricted to the transient portions of the stimulus are significantly orientation selective. However, that the orientation signal is strongest during the sustained portion of the stimulus seems to suggest that the coarser orientation signal conveyed by RA afferents interferes with the stronger SA1-mediated orientation signal [a result reminiscent of that shown by Bensmaia et al. (2006b)]. Another possibility is that the strong orientation signal observed during the sustained portion of the stimulus does not stem directly from convergent SA1 input but rather originates from intracortical processing (see Discussion).

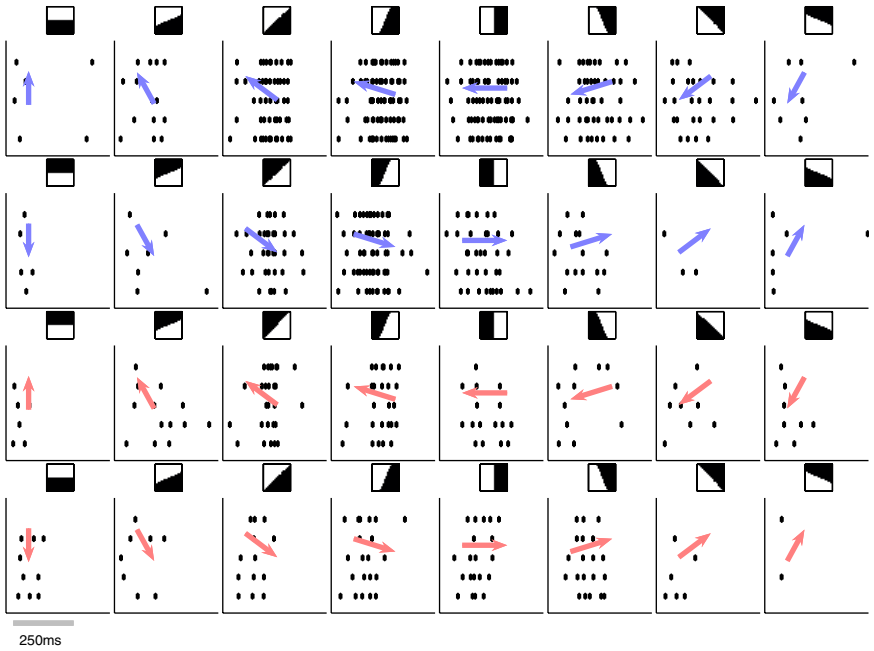

Figure 7. Response of a neuron in area 3b to scanned edges (shown as insets at the top of each raster). This neuron responded most strongly to bars oriented at 67.5° (Figs. 1, 2) and also responds preferentially to edges at this orientation. Furthermore, the responses to leading (blue arrows) edges are stronger and more strongly tuned than those to trailing edges (red arrows).

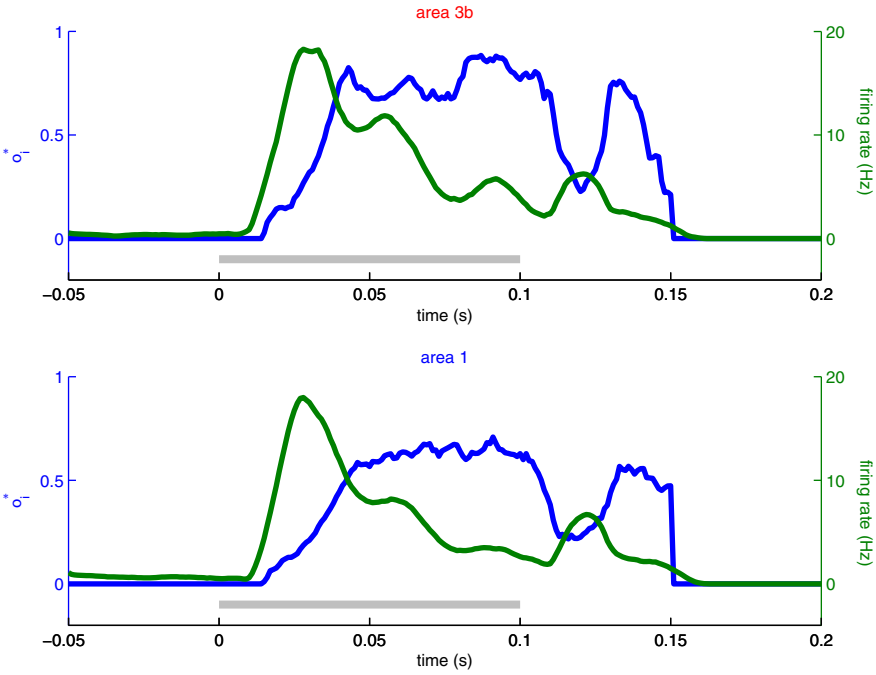

Figure 8. Time course of the response of significantly orientation-selective neurons to indented bars ($N_{\text{area 3b}} = 15$; $N_{\text{area 1}} = 30$). Mean response (green) and orientation selectivity index (blue) plotted as a function of time. The gray bar shows the time course of the stimulus. The orientation signal is weakest during the on- and off-responses, suggesting that the RA input conveys a weak orientation signal.

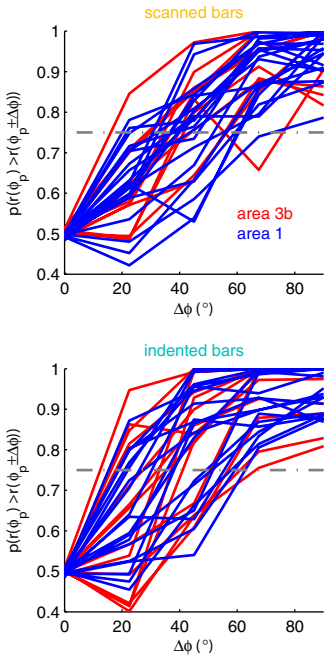

Figure 9. Neurometric functions derived from the responses to scanned (top) and indented (bottom) bars. For the sake of clarity, only data obtained from the most orientation-selective cells ($p < 0.001$) are shown. For scanned bars, 10 of 63 neurons in area 3b and 21 of 69 neurons in area 1 meet this orientation selectivity criterion; for indented bars, the proportions are 14 of 31 and 19 of 47 for areas 3b and 1, respectively. The angular thresholds for the most orientation-selective neurons, between 10 and 20°, are comparable with psychophysical angular thresholds.

Comparing psychophysical and neural angular thresholds

In a companion psychophysical study, we measured the discriminability of oriented bars identical with those presented in the neurophysiological experiments described here. The goal was to compare the perceptual discriminability of the stimuli with the discriminability of the responses they evoke in cortical neurons. We wanted to determine whether the representation of orientation in primary somatosensory cortex can account for psychophysical performance. The psychophysical threshold criterion was 75% correct discrimination and an analogous threshold was used for the neural thresholds. Figure 9 shows the neurometric functions derived from the responses of the most orientation-selective cells to scanned bars (for the sake of clarity, the criterion for o_i was set high to $p < 0.001$). As can be seen from the figure, the angular thresholds of the most orientation-selective neurons were between 10 and 20°. Because psychophysical angular thresholds were found to be between 15 and 25° as well, the orientation signal in primary somatosensory cortex can account for psychophysical performance.

Mechanisms of orientation selectivity

Next, we wanted to explore the neural mechanisms that underlie the orientation dependence of the responses of orientation-selective neurons. The most straightforward possibility is that these neurons receive convergent, linearly summing input from afferents whose RFs are organized eccentrically. According to this hypothesis, a linear filter should provide a reasonably good estimate of the neural responses. As a first approximation, we used the RF map measured using punctate probes as an estimate of the linear filter (Fig. 10, left panel). We found that this simple linear model accounted for, on average, only 30% of the variance in the responses of neurons in area 3b, and 20% of the variance in the responses of neurons in area 1 (Fig. 11*A*). The distribution of R^2, which can be thought of as an index of response linearity given this model, was identical for neurons that were orientation selective and for neurons that were not. This analysis suggests, then, that the mechanisms underlying orientation selectivity are different in areas 3b and 1 and are more linear with the displacement profile of the stimulus in the former than in the latter.

The poor fit of the simple linear model may be attributable to skin mechanics, which lead to a nonlinear transformation of the displacement profile even before transduction (Phillips and Johnson, 1981b; Sripati et al., 2006). The linearity indices obtained using strain profiles tended to be higher than those obtained using the displacement profiles, but not significantly so (Fig. 11*B*) (paired t test on Fischer's transforms of the correlations: $t_{(77)} = -0.95$, $p > 0.3$). Thus, the bulk of the nonlinearity in the neural response is not attributable to skin mechanics. The importance of skin mechanics in shaping the neural response is likely to be more significant for more complex stimuli than bars (e.g., spheres or gratings) (cf. Sripati et al., 2006).

One possible explanation for the relatively poor fit of these two models is that the measured punctate RF is a poor estimate of the linear RF that underlies the responses of the neuron. We therefore tested two other linear models in which the linear filter was characterized using a simple two-dimensional function. The first function we tested was the two-dimensional Gaussian (Fig. 10, top middle panel). According to this model, then, the RF of the neuron consists only of a bell-shaped excitatory region; the orientation selectivity of the neuron stems from the eccentricity of the RF: The RF is more elongated along one axis than along the perpendicular axis. The Gaussian model accounted for, on average, 62% of the variance in the responses of orientation-selective neurons in area 3b, and 49% of the variance in the responses of orientation-selective neurons in area 1 (Fig. 11*C*) (i.e., approximately twice that captured by the punctate-probe RF model).

The two-dimensional Gabor filter has been successfully used to model the responses of neurons in the primary visual cortex. The principal difference between this and the Gaussian model is that the excitatory region is flanked by inhibitory patches, which serve to strengthen the orientation tuning of the cells (Fig. 10, top right panel). We found that this model yielded better predictions than the Gaussian model (Fig. 11*D*), a difference reflected not only in the coefficient of determination (area 3b, $R^2 = 0.68$; area 1, $R^2 = 0.57$) but also, to some degree, in the Bayesian information criterion (BIC), an index of fit that penalizes free parameters (nine parameters for the Gabor model, seven for the Gaussian model): for area 3b neurons, the mean BICs were lower for Gabor than for Gaussian filters 67% of the time (a lower BIC indicates a better fit); for area 1 neurons, Gabor fits were better than Gaussian fits 57% of the time according to this criterion. However, Gabor filters yielded better BICs than Gaussian filters for 75% of the most orientation-selective neurons ($p < 0.001$; the proportion was equivalent in areas 3b and 1). Interestingly, the Gaussian and Gabor filters were better at predicting the responses of orientation-selective neurons in area 3b than they were at predicting the responses of neurons that were not orientation selective (Fig. 11*C*,*D*). This discrepancy may reflect a difference in the computations effected by these two populations of neurons.

As discussed above, some neurons were significantly orientation selective for scanned and indented bars, whereas others were only orientation selective for indented bars. One possibility is that neurons that exhibited significantly orientation-tuned responses for scanned bars were less linear in the afferent input than were neurons that were significantly tuned only for indented

bars. In fact, the opposite was true: The mean R^2 value was higher for neurons that were significantly tuned for orientation for both scanned and indented bars than it was for neurons that were significantly tuned only for indented bars. This difference was significant for the Gaussian ($t_{(42)} = 2.1$; $p < 0.05$) and Gabor ($t_{(42)} = 2.2$; $p < 0.05$) models but not for the two punctate-probe RF models.

The punctate RF map (Fig. 10, bottom left panel) was a much better predictor of afferent responses than it was of cortical responses (Fig. 11): the mean R^2 value was 0.77 for SA1 and 0.82 for RA afferents. Using the strain profile rather than the displacement profile yielded a slight improvement in model fit ($R^2 = 0.81$ and 0.84 for SA1 and RA afferents, respectively). The Gaussian and Gabor models yielded better predictions than did the punctate RF model, but the improvement was substantially less than that observed for cortical neurons (Fig. 11). Furthermore, the three linear filters (punctate RF, Gaussian, and Gabor) were very similar (Fig. 10, bottom panels).

From the above analyses, we conclude that the response of afferents is considerably more linear in the displacement profile than is that of cortical neurons, and the response of neurons in area 3b is more linear in the displacement profile (and thus in the afferent input) than is that of neurons in area 1. Second, a Gabor function captures a substantial amount of the variance in the response, particularly for neurons in area 3b. The better fit of the Gabor model relative to the Gaussian model suggests that orientation tuning is strengthened by inhibitory bands in somatosensory RFs, as has been found to be the case in the primary visual cortex. It is interesting to note that the neurons in area 3b for which the Gaussian or Gabor models did not provide a good fit were not orientation selective (Fig. 11*C*,*D*). This non-orientation-selective subpopulation of neurons may either be less linear than their orientation-selective counterparts, or may have linear RFs that are poorly approximated by Gaussian or Gabor filters.

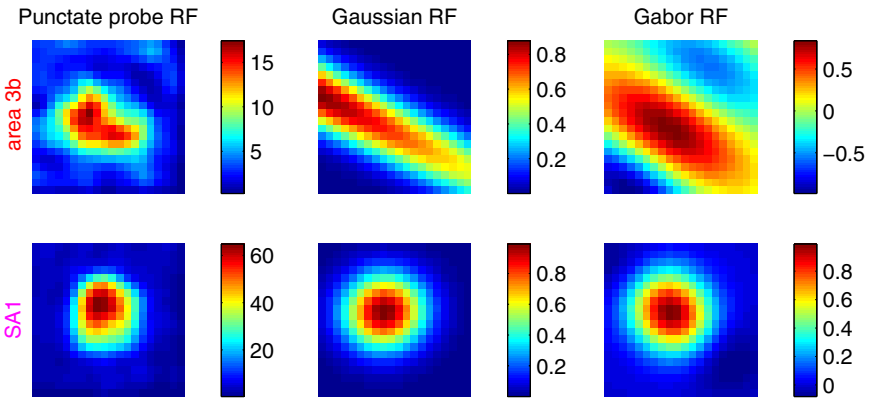

Figure 10. RFs for a highly orientation-selective neuron in area 3b (top) ($o_i = 0.54$; $p < 0.001$) and for an SA1 afferent (bottom) estimated using three methods. The first method consists of computing the mean responses to punctate probes; the second and third methods consist in fitting two-dimensional Gaussian and two-dimensional Gabor functions, respectively, to responses to bars (see text). Color shows the relative weight assigned to each pixel (see color bars for scale). For the cortical neuron, the model using the punctate RF accounted for 28% of the variance in the response of the neuron to indented bars, the Gaussian model accounted for 73% of the variance, and the Gabor model, 65%. For the afferent, the punctate RF model accounted for 80% of the variance (88% if the strain profile was used instead of the displacement profile), and the R^2 values for the Gaussian and Gabor models were 0.95.

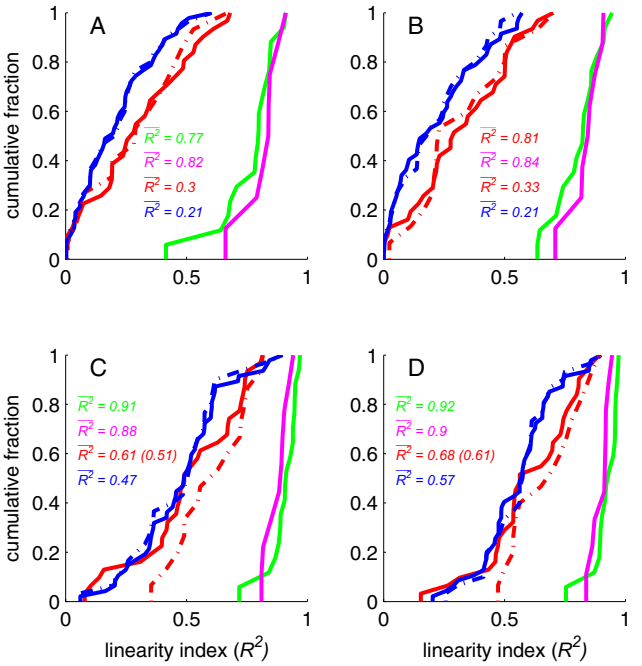

Figure 11. Distribution of the coefficients of determination for four linear filters. Magenta and green traces show the distribution of fits obtained from SA1 and RA responses, respectively; red and blue traces show the fits for neurons in areas 3b and 1, respectively. ***A***, Punctate probe RF map. ***B***, Punctate probe RF map using the strain profile. ***C***, Two-dimensional Gaussian filter. ***D***, Two-dimensional Gabor filter. The solid line shows the distribution for all the neurons, and the dashed lined shows the distribution for orientation-selective neurons ($p < 0.01$). The values of $\overline{R^2}$ in parentheses denote the mean coefficients of determination across the entire sample; all other values of $\overline{R^2}$ are for orientation-tuned cells only. The mean of the entire sample is shown only if it is significantly different from that of the orientation-selective sample. The responses of neurons in area 1 were significantly less linear with the displacement profile of the stimulus than were responses of neurons in area 3b.

Discussion

Orientation does not seem to be explicitly represented in the responses of single afferents but a large number of orientation detectors can be found in areas 3b and 1. Many neurons in both areas exhibit orientation tuning that is preserved across modes of stimulus presentation (scanned vs indented) and is relatively insensitive to other stimulus parameters, such as amplitude and speed, or to the nature of the stimulus, bar or edge. Orientation-selective neurons tend to be more SA-like than RA-like, and the strength of the orientation signal is strongest during the sustained portion of the response to an indented bar. The most orientation-selective neurons in SI are comparable in sensitivity to that measured in humans. Finally, responses of SI neurons to bars can be modeled with a high degree of accuracy using Gabor filters, similarly to their visual counterparts.

The contribution of SA1 and RA input to the representation of orientation selectivity

SA neurons tended slightly but significantly to be more orientation selective than RA neurons. Furthermore, the orientation signal was weakest during the on- and off-responses. The trough in the orientation signal during the off-response is particularly noteworthy because the off-response is likely the product of RA input alone because SA1 afferents do not exhibit off-responses. The burst of activity stemming from RA afferents thus seems to

interfere with the orientation signal in SI, likely stemming from input from SA1 fibers, which convey a sharper spatial image than do their RA counterparts (Fig. 4) (Phillips and Johnson, 1981a). The apparent interference of RA input in fine spatial processing has been observed in a previous study in which subjects judged the orientation of static and vibrating square-wave gratings (Bensmaia et al., 2006b). Sensitivity to grating orientation declined in proportion to the ratio of the RA to the SA1 response to the gratings [measured in a companion study: Bensmaia et al. (2006a)], and sensitivity improved after vibratory adaptation targeting the RA system.

Comparing the orientation representations in areas 3b and 1

Although we found a greater proportion of orientation-selective neurons in area 1 than in area 3b, particularly for scanned bars, the tuning strength of the most orientation-selective neurons in the two anatomical areas was similar. Despite the similarity in their orientation tuning, neurons in the two areas seem to be effecting different computations, as evidenced by the fact that the responses of neurons in area 1 are more poorly predicted using linear filters than are neurons in area 3b. One possibility is that area 1 neurons behave as more complex feature detectors than do area 3b neurons. For instance, many neurons in area 1 exhibit strong tuning for direction of motion in addition to orientation (data not shown), which may require more nonlinear processing (Gardner, 1984).

The abundance of orientation-selective neurons in areas 3b and 1 suggests that both cortical regions are involved in form processing. Both areas receive thalamic input from the ventrobasal complex of the thalamus, but area 1 also receives projections from area 3b, which suggests that area 1 lies at a higher processing stage than area 3b. Ablation studies show that animals without area 3b are unable to perform a wide range of tactile tasks, whereas animals with lesions of area 1 exhibit only mild deficits in simple form discrimination tasks (Randolph and Semmes, 1974). One possibility is that area 1 is involved in more complex form processing that is not taxed in the form discrimination tasks used in these studies.

Comparing psychophysics with neurophysiology

In a paired psychophysical study (Bensmaia et al., 2008), we characterized the ability of human observers to perceive the orientation of bars presented to the index finger. Using several methods, we estimated the mean angular threshold to be between 17 and 27°. By interpolating the neurometric functions obtained from significantly orientation-selective neurons, we estimated the angular thresholds (i.e., the angular separation that elicited different neural responses 75% of the time). For indented bars, we found the minimum angular threshold to be 8° for neurons in area 3b and 14° for neurons in area 1. For scanned bars, the lowest angular thresholds were 14 and 23° for neurons in areas 3b and 1, respectively. Thus, the fidelity of the orientation signal conveyed by the most orientation-selective cell in the primary somatosensory cortex can account for psychophysical performance. From the perspective of an ideal observer, in fact, the orientation signal in SI is perhaps more refined than is the perception of orientation.

In the psychophysical experiments, we also found orientation sensitivity to be more or less independent of the presentation mode (scanned vs indented) and of the stimulus type (bar vs edge); angular thresholds were also insensitive to changes in stimulus parameters (amplitude and scanning speed). The perceptual constancy of orientation across stimulus conditions matches the relative insensitivity of neural orientation sensitivity to these same stimulus manipulations.

Neural mechanisms of orientation selectivity

DiCarlo and Johnson (2000) derived linear RFs for neurons in area 3b from responses to scanned random dot patterns using reverse correlation. RFs were found to consist of a central excitatory region flanked by one or more inhibitory ones. A model consisting of three Gaussian filters, the first corresponding to the excitatory center, the other two to inhibitory lobes (the first appearing simultaneously with the excitatory center, the second temporally lagged with respect to it) accounted for much of the structure in the measured RFs. Furthermore, orientation sensitivity was found to be most dependent on the excitatory and fixed inhibitory lobes. Because the Gabor filter describes an excitatory mass flanked by an inhibitory one, the Gabor model is analogous to DiCarlo and Johnson's model (but with fewer degrees of freedom).

That the RFs derived from responses to punctate probes and RFs derived from responses to indented bars are different (Fig. 10) suggests that these RFs are each linear approximations to nonlinear mechanisms: the dramatic difference in RFs is attributable to the difference in the stimuli used to obtain them. Note that responses of mechanoreceptive afferents to indented bars are well predicted using the punctate RFs as linear filters, and more complex models yield only slightly better predictions. Thus, afferent responses to indented bars are relatively linear in the displacement profile, in contrast to their cortical counterparts. There seems to be a progressive tendency, then, for responses to become more nonlinear as one ascends the perceptual pathway: Afferent responses are most linear, followed by responses of neurons in area 3b, and then by those of neurons in area 1 (Fig. 11).

The question remains what neural mechanisms underlie this orientation selectivity. According to the classical theory of orientation selectivity in primary visual cortex (V1) (Hubel and Wiesel, 1962), the orientation selectivity of simple cells in V1 stems from the arrangement of their thalamic inputs: the receptive fields of neurons in the lateral geniculate nucleus that send projections to individual simple cells are arranged linearly so that the input is tuned for bars that fall within the aligned RFs. The feedforward model has been extensively elaborated on both theoretically and empirically (for review, see Ferster and Miller, 2000). An alternative theory is that, although the thalamic input to a simple cell is broadly tuned for orientation, the bulk of its orientation tuning is effected through intracortical processing (Sompolinsky and Shapley, 1997).

The results presented here do not explicitly address these issues of neural mechanisms. However, the orientation tuning observed in SI is in some respects similar to its visual counterpart. First, the tuning strength observed in orientation-selective neurons in SI overlapped to a large degree with that observed in V1 neurons of macaque: Ringach et al. (2002) found the mean o_i to be 0.4 in V1, whereas the mean o_i for (significantly orientation-selective) SI neurons was 0.26. (Ringach et al. used circular variance, which is $1 - o_i$.) The main difference between the distribution of o_i in primary visual and somatosensory cortices was that o_i was essentially uniformly distributed in V1, whereas the distribution is strongly positively skewed in SI, so V1 contains a larger proportion of strongly tuned neurons than does SI. Second, a striking similarity between the two modalities is the invariance of tuning with respect to stimulus amplitude, which is analogous to the contrast invariance of the tuning of simple cells in primary visual cortex. Contrast invariance cannot be explained by simple

feedforward mechanisms, but rather requires either intracortical processing (Sompolinsky and Shapley, 1997) or a specialized feedforward circuitry such as "push–pull" inhibition (Ferster and Miller, 2000). Thus, although little is known of the mechanisms of orientation tuning in somatosensory cortex, it seems to be similar in its properties to orientation tuning in vision. The two phenomena may thus be mediated by analogous neural mechanisms.

References

Bensmaia SJ, Craig JC, Yoshioka T, Johnson KO (2006a) SA1 and RA afferent responses to static and vibrating gratings. J Neurophysiol 95:1771–1782.

Bensmaia SJ, Craig JC, Johnson KO (2006b) Temporal factors in tactile spatial acuity: evidence for RA interference in fine spatial processing. J Neurophysiol 95:1783–1791.

Bensmaia SJ, Hsiao SS, Denchev PV, Killebrew JH, Craig JC (2008) The tactile perception of stimulus orientation. Somatosens Mot Res, in press.

Darian-Smith I, Kenins P (1980) Innervation density of mechanoreceptive fibers supplying glabrous skin of the monkey's index finger. J Physiol (Lond) 309:147–155.

DiCarlo JJ, Johnson KO (2000) Spatial and temporal structure of receptive fields in primate somatosensory area 3b: effects of stimulus scanning direction and orientation. J Neurosci 20:495–510.

Ferster D, Miller KD (2000) Neural mechanisms of orientation selectivity in the visual cortex. Annu Rev Neurosci 23:441–471.

Freeman AW, Johnson KO (1982) Cutaneous mechanoreceptors in macaque monkey: temporal discharge patterns evoked by vibration, and a receptor model. J Physiol (Lond) 323:21–41.

Gardner EP (1984) Cortical neuronal mechanisms underlying the perception of motion across the skin. In: Somatosensory mechanisms (von Euler C, Franzén O, Lindblom U, Ottoson D, eds), pp 93–112. London: Macmillan.

Hsiao SS, Bensmaia SJ (2007) Coding of object shape and texture. In: Handbook of the senses (Kaas JH, Basbaum AI, eds). New York: Elsevier.

Hsiao SS, Lane JW, Fitzgerald P (2002) Representation of orientation in the somatosensory system. Behav Brain Res 135:93–103.

Hubel DH, Wiesel TN (1962) Receptive fields, binocular interaction and functional architecture in the cat's visual cortex. J Physiol (Lond) 160:106–154.

Hyvärinen J, Poranen A (1978) Movement-sensitive and direction and orientation-selective cutaneous receptive fields in the hand area of the post-central gyrus in monkeys. J Physiol (Lond) 283:523–537.

Johansson RS, Vallbo ÅB (1979) Tactile sensibility in the human hand: relative and absolute densities of four types of mechanoreceptive units in glabrous skin. J Physiol (Lond) 286:283–300.

Johnson KO, Lamb GD (1981) Neural mechanisms of spatial tactile discrimination: neural patterns evoked by Braille-like dot patterns in the monkey. J Physiol (Lond) 310:117–144.

Killebrew JH, Bensmaïa SJ, Dammann JF, Denchev P, Hsiao SS, Craig JC, Johnson KO (2006) A dense array stimulator to generate arbitrary spatio-temporal tactile stimuli. J Neurosci Methods 161:62–74.

LaMotte RH, Srinivasan MA (1987a) Tactile discrimination of shape: responses of slowly adapting mechanoreceptive afferents to a step stroked across the monkey fingerpad. J Neurosci 7:1655–1671.

LaMotte RH, Srinivasan MA (1987b) Tactile discrimination of shape: responses of rapidly adapting mechanoreceptive afferents to a step stroked across the monkey fingerpad. J Neurosci 7:1672–1681.

Mardia KV (1972) Statistics of directional data. London: Academic.

Mountcastle VB, Reitboeck HJ, Poggio GF, Steinmetz MA (1991) Adaptation of the Reitboeck method of multiple microelectrode recording to the neocortex of the waking monkey. J Neurosci Methods 36:77–84.

Phillips JR, Johnson KO (1981a) Tactile spatial resolution: II. Neural representation of bars, edges, and gratings in monkey primary afferents. J Neurophysiol 46:1192–1203.

Phillips JR, Johnson KO (1981b) Tactile spatial resolution: III. A continuum mechanics model of skin predicting mechanoreceptor responses to bars, edges, and gratings. J Neurophysiol 46:1204–1225.

Pubols LM, Leroy RF (1977) Orientation detectors in the primary somatosensory neocortex of the raccoon. Brain Res 129:61–74.

Randolph M, Semmes J (1974) Behavioral consequences of selective ablations in the postcentral gyrus of *Macaca mulatta*. Brain Res 70:55–70.

Ringach DL, Shapley RM, Hawken MJ (2002) Orientation selectivity in macaque V1: diversity and laminar dependence. J Neurosci 22:5639–5651.

Sompolinsky H, Shapley R (1997) New perspectives on the mechanisms for orientation selectivity. Curr Opin Neurobiol 7:514–522.

Srinivasan MA, LaMotte RH (1987) Tactile discrimination of shape: responses of slowly and rapidly adapting mechanoreceptive afferents to a step indented into the monkey fingerpad. J Neurosci 7:1682–1697.

Sripati AP, Bensmaia SJ, Johnson KO (2006) A continuum mechanical model of mechanoreceptive afferent responses to indented spatial patterns. J Neurophysiol 95:3852–3864.

Talbot WH, Darian-Smith I, Kornhuber HH, Mountcastle VB (1968) The sense of flutter-vibration: comparison of the human capacity with response patterns of mechanoreceptive afferents from the monkey hand. J Neurophysiol 31:301–334.

Vallbo ÅB, Johansson RS (1978) The tactile sensory innervation of the glabrous skin of the human hand. In: Actice touch. The mechanism of recognition of objects by manipulation: a multi-disciplinary approach (Gordon G, ed), pp 29–54. Oxford: Pergamon.

Warren S, Hämäläinen HA, Gardner EP (1986) Objective classification of motion- and direction-sensitive neurons in primary somatosensory cortex of awake monkeys. J Neurophysiol 56:598–622.